Research article

polymers advanced technologies

Received: 12 August 2015, Revised: 11 September 2015, Accepted: 11 September 2015, Published online in Wiley Online Library: 5 November 2015

(wileyonlinelibrary.com) DOI: 10.1002/pat.3699

Anthracene-thieno[3,4-*c*]pyrrole-4,6-dione based donor–acceptor conjugated copolymers for applications in optoelectronic devices

Luke Cartwright, Thomas J. Neal, Nathan J. Rutland and Ahmed Iraqi*

Three novel alternating copolymers of thieno[3,4-*c*]pyrrole-4,6-dione (TPD) and triisopropylsilylacetylene-functionalized anthracene were prepared via Suzuki polymerization. Various solubilizing substituents were attached to the TPD moiety in order to ascertain the impact they have upon the optical, electrochemical, and thermal properties of the resulting polymers. All copolymers showed good solubility and thermal stability with decomposition temperatures in excess of 300°C. Optical properties revealed that PTATPD(O), PTATPD(DMO), and PTATPD(BP) displayed optical energy gaps in excess of 2.0 eV. It is speculated that steric repulsion between solubilizing groups on repeat units along polymer chains reduces their planarity and decreases their electronic conjugation. The amorphous nature of the polymers was confirmed with differential scanning calorimetry and powder X-ray diffraction. The highest occupied molecular orbital levels of the three polymers are unaffected by the different solubilizing chains. However, they exert some influence over the lowest unoccupied molecular orbital (LUMO) levels with PTATPD(BP) and PTATPD(O) displaying the lowest LUMO levels (−3.4 eV). In contrast, PTATPD(DMO) displayed the highest LUMO level (−3.3 eV). © 2015 The Authors. *Polymers for Advanced Technologies* Published by John Wiley & Sons Ltd.

Supporting information may be found in the online version of this paper.

Keywords: conjugated polymers; optoelectronics; optical properties; anthracene; thieno[3,4-c]pyrrole-4,6-dione

INTRODUCTION

Semiconducting polymers offer distinct advantages over their inorganic counterparts including the following: light weight, improved mechanical flexibility, large active layers, and can be manufactured using low-cost solution processing.[1,2] It is hypothesized that conjugated polymers will fulfill a larger number of functions providing large-scale industrial manufacture of organic electronics becomes feasible.[1] In actuality, the commercial success of organic light-emitting diodes (OLEDs) should serve as a platform to promote the efficacy of organic optoelectronic devices.[3–6] Aside from OLEDs, the electrical, magnetic, and optical properties of conjugated polymers makes them promising candidates for organic photovoltaic devices, organic field-effect transistors, electrochromic devices, and stable electronic memories on flexible circuit boards.[7–15] Furthermore, they have proven to be suitable candidates for gas and humidity sensing and bio-sensing, which can be attributed to their sensitivity to biological, chemical, and physical perturbations.[16,17]

The attractiveness of conjugated polymers lies in the facile tunability of their optical, electronic, and morphological properties.[18] Previous literature has proven that copolymerising an electron-rich donor monomer with an electron-deficient acceptor unit in a so-called donor-π-acceptor (D-π-A) arrangement is an effective method of tuning these properties.[19–21] The alternation of donor and acceptor units results in hybridization of the lowest unoccupied molecular orbital (LUMO) of the acceptor and highest occupied molecular orbital (HOMO) of the donor, resulting in a decreased band gap.[12] Moreover, it is believed that the D-π-A arrangement promotes intramolecular charge transfer along the polymer backbone, which can enhance charge carrier mobility.[12] This D-π-A methodology has been used to produce a range of conjugated chromophores that absorb light over the whole solar spectrum.

Literature reports have speculated that the highly planar and symmetrical structure of thieno[3,4-*c*]pyrrole-4,6-dione (TPD) repeat units along polymer chains could improve electron delocalization thereby enhancing interchain interactions and increasing their hole mobility.[22,23] Furthermore, the nitrogen of the imide functionality can be substituted with solubilizing groups, facilitating solution processing of the final polymer. Finally, the electron-withdrawing nature of the TPD moiety allows it, once polymerized with alternate electron donor units, to form the highly desirable D-π-A arrangement. There is currently a large body of work covering the use of TPD in optoelectronic devices, mainly in photovoltaic devices and organic field-effect transistors.[22–26] TPD-based copolymers have displayed efficiencies up to 8% when fabricated into a bulk heterojunction solar cell using $PC_{70}BM$ as the acceptor.[27] Additionally, TPD-containing copolymers have displayed high hole mobilities (1.29 cm^2/Vs) when fabricated into field-effect transistors.[28]

2,6-Linked anthracene units are finding use in D-π-A conjugated polymers.[29–33] Iraqi and co-workers presented the

* *Correspondence to: Ahmed Iraqi, Department of Chemistry, University of Sheffield, Sheffield S3 7HF, UK.*
E-mail: a.iraqi@sheffield.ac.uk

L. Cartwright, T. J. Neal, N. J. Rutland, A. Iraqi
Department of Chemistry, University of Sheffield, Sheffield S3 7HF, UK

preparation of D-π-A polymers with alternating 2,6-linked anthracene units with aryloxy substituents at their 9,10-positions and various benzothiadiazole alternate repeat units.[33] Bulk heterojunction solar cells fabricated from these polymers displayed efficiencies ranging from 1.93% to 4.17% when blended with $PC_{70}BM$.[33]

Copolymers comprising alternating benzo[1,2-*b*:4,5-*b*']dithiophene units and electron-donating units have been reported in literature.[34–37] However, to the best of our knowledge, nobody has reported any alternating TPD-anthracene copolymers. In the present contribution, we report the synthesis of three alternating copolymers comprising TPD with varying substituents as electron-accepting moieties and triisopropylsilylacetylene-functionalized anthracene as electron-donor moieties. The preparation of polymers **PTATPD**(**O**), **PTATPD**(**DMO**), and **PTATPD**(**BP**) (Fig. 1) is presented along with a study of their optical, electrochemical, thermal, and structural properties.

RESULTS AND DISCUSSION

Polymer synthesis

The synthetic route for the preparation of the three TPD monomers is outlined in Scheme 1. It is perhaps worth mentioning that **M2** and **M3** were obtained in slightly lower yields, relative to **M1**. This was attributed to the additional steric hindrance associated with 3,7-dimethyloctan-1-amine and 4-butylaniline. The structures of **PTATPD**(**O**), **PTATPD**(**DMO**), and **PTATPD**(**BP**) are outlined in Fig. 1. Suzuki polycondensation of **M1** with **M4**, **M2** with **M4**, and **M3** with **M4** yielded **PTATPD**(**O**), **PTATPD**(**DMO**), and **PTATPD**(**BP**), respectively. $Pd(OAc)_2$ and tri(*o*-tolyl)phosphine were used as the catalyst and sodium hydrogen carbonate as the base. All polymerizations were left for 24 hr with large quantities of bright red precipitate forming. The polymers were fractionated via Soxhlet extraction using methanol, acetone, hexane, and toluene. The toluene fractions were collected, reduced *in vacuo*, and precipitated in methanol. Subsequent studies were conducted on the toluene fractions only. The chemical structures of **PTATPD**(**O**), **PTATPD**(**DMO**), and **PTATPD**(**BP**) were confirmed via ^{1}H nuclear magnetic resonance (NMR) (supplementary information) and elemental analysis. The number-average molecular weight (M_n) and weight-average molecular weight (M_w) were estimated using gel permeation chromatography (GPC) using 1,2,4-trichlorobenzene as the eluent at 140°C (Table 1). Substituting *n*-octyl chains in **PTATPD**(**O**) for dimethyloctyl chains in **PTATPD**(**DMO**) on the TPD moiety results in a significantly higher M_w. It is speculated that the branched alkyl chain disrupts intermolecular interactions in solution, increasing the solubility of the resulting polymer. Thus, the final polymer product is able to achieve a higher M_w before precipitating out of solution. **PTATPD**(**BP**) displays a higher M_w (97,700 Da) relative to **PTATPD**(**O**) (74,600 Da). However, the M_n of **PTATPD**(**BP**), and **PTATPD**(**O**) are 25,900 and 27,300 Da, respectively. Thus, **PTATPD**(**BP**) has a significantly wider distribution of molecular weights, relative to **PTATPD**(**O**).

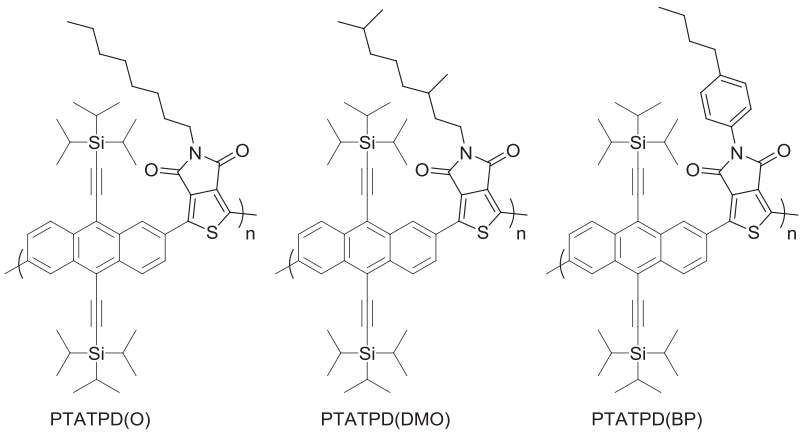

Figure 1. Structures of **PTATPD**(**O**), **PTATPD**(**DMO**), and **PTATPD**(**BP**).

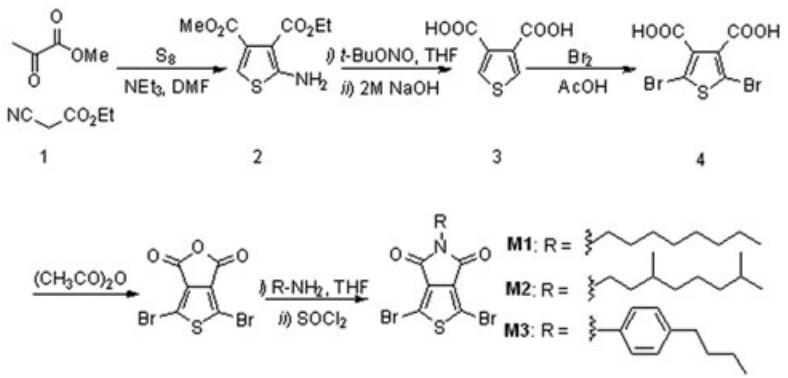

Scheme 1. Synthetic route towards the TPD monomers **M1**, **M2**, and **M3**.

Table 1. A summary of the GPC, UV–vis absorption, and photoluminescence data for **PTATPD**(**O**), **PTATPD**(**DMO**), and **PTATPD**(**BP**)

Polymer	M_w (Da)[a]	PDI	UV–vis absorption λ_{max} Solution (nm)	UV–vis absorption ε (M^{-1} cm^{-1})[b]	UV–vis absorption λ_{max} film (nm)	UV–vis absorption E_g^{opt} film (eV)[c]	Photoluminescence λ_{max} solution (nm)	Photoluminescence λ_{max} film (nm)	Stokes shift (nm)[d]
PTATPD(**O**)	74,600	2.73	383, 529	62,500	388, 548	2.16	545	617	69
PTATPD(**DMO**)	106,700	2.61	383, 533	61,300	390, 553	2.14	544	619	66
PTATPD(**BP**)	97,700	3.77	383, 532	62,000	389, 550	2.12	552	629	79

[a]Measurements conducted on the toluene fraction of the polymer using DRI detection.
[b]Absorption coefficient measured at λ_{max} = 383 nm in chloroform solution.
[c]Optical energy gap determined from the onset of the absorption band in thin film.
[d]Stokes shift determined from film studies.
GPC, gel permeation chromatography; UV–vis, ultraviolet–visible; DRI, differential refractive index.

Optical properties

The ultraviolet–visible absorption properties of the polymers were investigated in solution and film state (Fig. 2). The results are summarized in Table 1. All polymers display an intense transition band at 383 nm in solution, corresponding to a π-π^* transition. This band is red-shifted to 388, 390, and 389 nm for **PTATPD**(**O**), **PTATPD**(**DMO**), and **PTATPD**(**BP**), respectively, in films states. **PTATPD**(**O**), **PTATPD**(**DMO**), and **PTATPD**(**BP**) display a second, less intense transition at 529, 533, and 532 nm in solution, respectively. This is red-shifted to 548, 553, and 550 nm for **PTATPD**(**O**), **PTATPD**(**DMO**), and **PTATPD**(**BP**) in film states, respectively. This transition corresponds to intramolecular charge transfer between the TPD-acceptor unit and the anthracene-donor moiety. The small bathochromic shift (~20 nm) that is observed from solution to films indicates that the polymers adopt a similar conformation in both states. The optical band gaps, as estimated from the onset of absorption wavelengths, are 2.16, 2.14, and 2.12 eV for **PTATPD**(**O**), **PTATPD**(**DMO**), and **PTATPD**(**BP**), respectively.

The results indicate that the optical properties of the polymers are not significantly affected by the molecular weight or the nature of the substituent attached to the TPD moiety. It is speculated that there is a large torsion angle between the anthracene moiety and the TPD unit, arising from the intramolecular repulsion between the bulky TIPS group and functionalized-imide on the TPD. Consequently, the planarity of the polymer is disrupted. Thus, orbital overlap between non-coplanar aromatics is poor, leading to localization of the π-electron wave functions and a decreased electronic conjugation. Therefore, the true effects the different substituents have on the optical properties are not revealed. It is hypothesized that the lack of a regular, planar structure will result in an amorphous polymer.

Najari and co-workers synthesized a series of thieno[3,4-*c*]pyrrole-4,6-dione-*alt*-2,7-carbazole polymers. The lowest optical band gap reported by the group was 1.97 eV. They speculated that the alkyl chains twist the polymer backbone decreasing the effective conjugation length resulting in a wider optical band gap.[38]

The homopolymer, regioregular poly(3-hexylthiophene-2,5-diyl) (**P3HT**), displays a reduced optical band gap of 1.9 eV and a larger bathochromic shift from solution to film.[39,40] It is hypothesized that the localization of the π-electron wavefunction, decreased electronic conjugation, and amorphous nature of the polymers synthesized in this report are responsible for the wider optical band gaps, relative to **P3HT**. Furthermore, it is known that the solar harvesting of **P3HT** is restricted by its mismatch with the solar spectrum.[39,40] The optical band gaps of **PTATPD**(**O**), **PTATPD**(**DMO**), and **PTATPD**(**BP**) are wider than that of **P3HT**. Thus, these polymers are not optimized with respect to the maximum photon flux of the solar spectrum.

The photoluminescence (PL) emission spectra of the polymers in solution and solid films are illustrated in Fig. 2. The PL spectra of all polymers in chloroform solution and thin films were excited at incident wavelengths of their absorption λ_{max}. In solution,

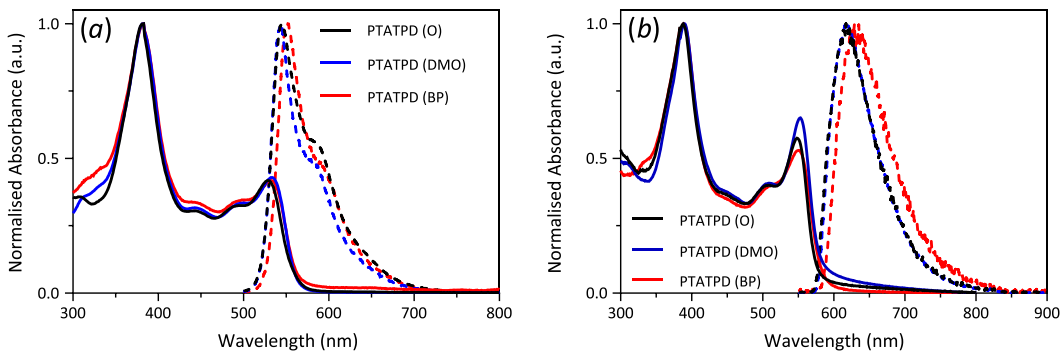

Figure 2. Normalized absorption spectra (full line) and photoluminescence spectra (dashed line) of **PTATPD**(**O**), **PTATPD**(**DMO**), and **PTATPD**(**BP**) in: (a) chloroform solution and (b) thin films. This figure is available in colour online at wileyonlinelibrary.com/journal/pat

PTATPD(O), **PTATPD(DMO)**, and **PTATPD(BP)** exhibit emission maximums at 545, 544, and 552 nm, respectively. Interestingly, all polymers display a shoulder peak in their solution PL spectra. We tentatively attribute this to an unresolved vibrational-electronic transition. The emission maxima are red-shifted to 617, 619, and 629 nm for **PTATPD(O)**, **PTATPD(DMO)**, and **PTATPD(BP)**, respectively, in solid state. The small Stokes shift of 69, 66, and 79 nm, respectively, indicates that there is a small energy difference between the ground state and excited states of the polymers.

Electrochemical properties

Cyclic voltammetry was used to characterize the frontier energy levels of the three polymers. The cyclic voltammograms on drop cast films in tetrabutylammonium perchlorate acetonitrile solutions of **PTATPD(BP)**, **PTATPD(O)**, and **PTATPD(DMO)** display irreversible oxidation peaks (Fig. 3). It is hypothesized that oxidation of the polymer yields a radical cation state localized on the imide moiety, which undergoes an irreversible chemical transformation. In contrast, the reduction peaks of all polymers are quasi-reversible. The energy levels of all polymers were estimated from the onset of the oxidation and reduction potentials. **PTATPD(BP)**, **PTATPD(O)**, and **PTATPD(DMO)** display the same HOMO level (−5.9 eV). The results indicate that incorporation of different substituents on the imide functionality does not alter the HOMO level of the resulting polymer. However, it does have a slight influence on the LUMO level of the resulting polymer. **PTATPD(DMO)** displays the highest LUMO level (−3.3 eV). In comparison, **PTATPD(BP)** and **PTATPD(O)** display a lower LUMO level (−3.4 eV). The results suggest that attaching different substituents to the imide functionality can subtly perturb the electron density on the main polymer chain.

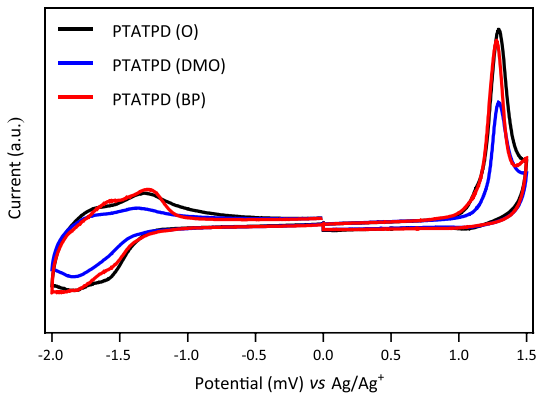

Figure 3. Cyclic voltammograms of **PTATPD(O)**, **PTATPD(DMO)**, and **PTATPD(BP)**. This figure is available in colour online at wileyonlinelibrary.com/journal/pat

The electrochemical band gap of the polymers is significantly larger than their corresponding optical band gap. It is believed that the additional energy is the result of the strong Coulomb attraction of excitons, which needs to be overcome in order to generate free charge carriers.

Previous literature has estimated the HOMO levels of **P3HT** and **PCPDTBT** to be −5.0 and −5.3 eV, respectively.[39,40] All polymers synthesized within this report display deeper HOMO levels than **P3HT** and **PCPDTBT**. Furthermore, all polymers synthesized in this contribution demonstrate significantly deeper HOMO levels than the polymers synthesized by Najari and co-workers.[38]

Thermal properties

Thermogravimetric analysis of **PTATPD(BP)**, **PTATPD(O)**, and **PTATPD(DMO)** revealed that all polymers possess good thermal stability with degradation temperatures (5% weight loss) occurring at 354°C, 360°C, and 309°C, respectively (Fig. 4a, Table 2). Differential scanning calorimetry (DSC) revealed that **PTATPD(O)** and **PTATPD(BP)** exhibit a broad, weak glass transition temperature (T_g) at 56.4°C and 48.4°C, respectively (Fig. 4b, Table 2). No polymers exhibited any clear melting endotherms up to 220°C on the DSC thermograms. This result supports the hypothesis that the polymers adopt an amorphous structure in the solid state.

The results obtained suggest that the thermal properties of the conjugated polymers are influenced by the size of the pendant group attached to the imide functionality, the larger the group the lower the T_d and T_g. **PTATPD(DMO)** and **PTATPD(BP)** display lower T_d and T_g temperatures relative to **PTATPD(O)**. We tentatively hypothesize that the larger groups create "free volume" within the polymer by increasing separation between polymer chains, allowing the polymer to reorganize more easily within solid state resulting in lower T_d and T_g temperatures.

Powder X-ray diffraction

Powder x-ray diffraction patterns of polymers **PTATPD(O)**, **PTATPD(DMO)** and **PTATPD(BP)** were obtained to investigate the molecular organization of polymers in solid state (Fig. 5). The X-ray diffraction (XRD) patterns of all polymers display a single broad diffuse feature, which is consistent with the random scatter of an amorphous solid. Furthermore, the lack of a peak

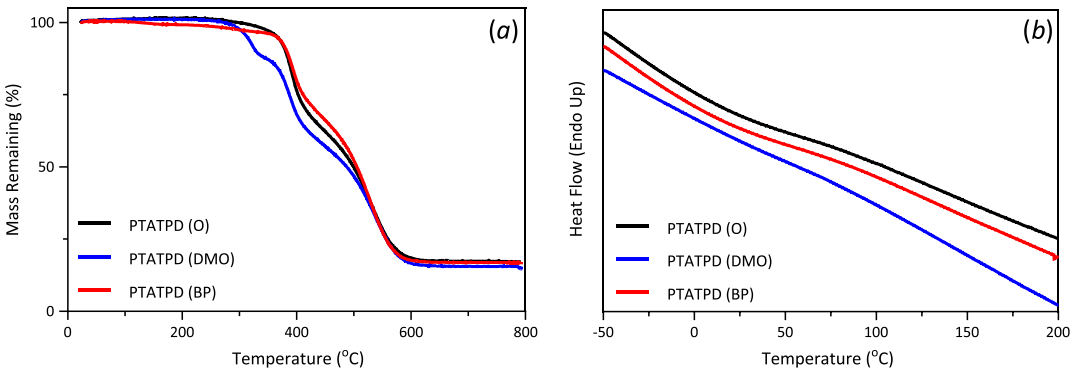

Figure 4. (a)Thermogravimetric analysis and (b) differential scanning calorimetry plots of **PTATPD(O)**, **PTATPD(DMO)**, and **PTATPD(BP)** with a heating rate of 10°C min^{-1} under an inert atmosphere of nitrogen. This figure is available in colour online at wileyonlinelibrary.com/journal/pat

Table 2. A summary of the TGA, DSC, and electrochemical data for **PTATPD**(**O**), **PTATPD**(**DMO**), and **PTATPD**(**BP**)

Polymer	T_g (°C)[a]	T_d (°C)[b]	HOMO (eV)[c]	LUMO (eV)[d]	E_g^{elec} (eV)[e]
PTATPD(**O**)	56.4	360	−5.9	−3.4	2.5
PTATPD(**DMO**)	—	309	−5.9	−3.3	2.6
PTATPD(**BP**)	48.4	354	−5.9	−3.4	2.5

[a]Glass transition temperature as measured by DSC.
[b]Onset of degradation as determined via TGA with a heating rate of 10°C min^{-1} under an inert atmosphere of nitrogen.
[c]HOMO position (versus vacuum) determined from the onset of oxidation.
[d]LUMO position (versus vacuum) determined from the onset of reduction.
[e]Electrochemical energy gap.
DSC, differential scanning calorimetry; TGA, thermogravimetric analysis; HOMO, highest occupied molecular orbital; LUMO, lowest unoccupied molecular orbital.

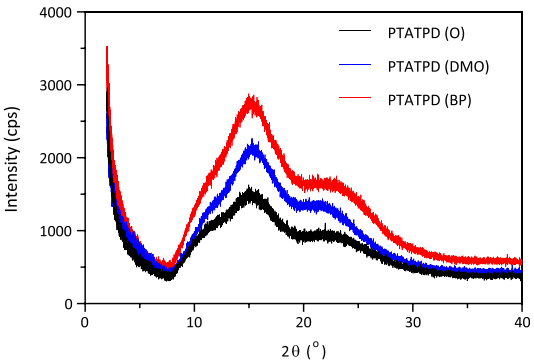

Figure 5. Powder X-ray diffraction patterns of **PTATPD**(**O**), **PTATPD**(**DMO**), and **PTATPD**(**BP**). This figure is available in colour online at wileyonlinelibrary.com/journal/pat

in the low angle region suggests that the polymer does not possess any long-range translational order; providing further evidence that the polymer has an amorphous structure in solid state. The results obtained from the XRD patterns agree with the DSC data.

CONCLUSIONS

In summary, the preparation of three alternating copolymers comprising TPD functionalized units and 9,10-bis(triisopropylsilylacetylene) anthracene units using Suzuki cross-coupling reactions was reported and yielded the polymers **PTATPD**(**O**), **PTATPD**(**DMO**), and **PTATPD**(**BP**). Their optical, thermal, electrochemical, and structural properties in solid state were characterized. The amorphous nature of the polymers was confirmed by DSC and powder XRD studies. It has been demonstrated that the M_w, electronic, and thermal properties are dependent upon the pendant-group attached to the TPD-moiety. The larger the pendant group, the higher the M_w and lower the T_d. Surprisingly, the optical properties, largely the absorption profiles, were not influenced by the pendant-group attached to the TPD-moiety. It is speculated that the intramolecular repulsion between solubilizing groups within the polymer reduces the planarity and decreases the electronic conjugation. Thus, changing the pendant-group has little impact on the optical properties of the resulting polymer.

EXPERIMENTAL

All materials were purchased from commercial suppliers and used as received, unless otherwise stated. Toluene was dried and distilled over sodium under an inert argon atmosphere. Acetonitrile was dried and distilled over phosphorous pentoxide under an inert argon atmosphere, then stored over molecular sieves (3 Å). 1,3-Dibromo-5-(n-octyl)-4H-thieno[3,4-c]pyrrole-4,6(5H)-dione (**M1**)[41], 1,3-dibromo-5-(3,7-dimethyloctyl)-4H-thieno[3,4-c]pyrrole-4,6(5H)-dione (**M2**),[42] and 2,6-dibromo-9,10-bis(triisopropylsilylacetylene)anthracene[43] were prepared according to literature procedures.

Measurements

^{1}H and ^{13}C NMR spectra were recorded on a Bruker AV 400 (400 MHz) using chloroform-d ($CDCl_3$) or acetone-d as the solvent. ^{1}H NMR spectra of the polymers were recorded on a Bruker Avance III HD 500 (Bruker, Coventry, United Kingdom) (500 MHz) spectrometer at 100°C using 1,2-dideutrotetrachloroethance ($C_2D_2Cl_4$) as the solvent. Coupling constants are given in Hertz (Hz). Carbon, hydrogen, nitrogen, and sulfur elemental analysis was performed on a Perkin Elmer 2400 series 11 CHNS/O analyzer (Perkin Elmer, Buckingham shire, United Kingdom). Analysis of halides was undertaken using the Schöniger flask combustion method. GPC analysis was conducted on polymer solutions using 1,2,4-trichlorobenzene at 140°C as the eluent. Polymer samples were spiked with toluene as a reference. GPC curves were obtained using a Viscotek GPCmax VE2001 GPC solvent/sample module and a Waters 410 Differential Refractometer (Waters, Hertfordshire, United Kingdom), which was calibrated using a series of narrow polystyrene standards (Polymer Laboratories). Thermogravimetric analyses (TGAs) were obtained using a Perkin Elmer TGA-1 Thermogravimetric Analyzer (Perkin Elmer, Buckinghamshire, United Kingdom) at a scan rate of 10°C min^{-1} under an inert nitrogen atmosphere. DSCs were obtained using a Perkin-Elmer Pyris 1DSC (Perkin Elmer, Buckinghamshire, United Kingdom) in the temperature range −50–220°C. Powder X-ray diffraction samples were recorded on a Bruker D8 advance diffractometer (Bruker, Coventry, United Kingdom) with a CuKα radiation source (1.5418 Å, rated as 1.6 kW). The scanning angle was conducted over the range 2–40°. Ultraviolet–visible absorption spectra were recorded using a Hitachi U-2010 Double Bean UV/Visible Spectrophotometer (Hitachi, Berckshire, United Kingdom). Polymer solutions were made using chloroform and measured using quartz cuvettes (path length = 1×10^{-2} m). Thin films, used for absorption spectra, were prepared by drop-casting solutions onto quartz plates using 1 mg cm^{-3} polymer solutions that were prepared with chloroform. Photoluminescence spectra were recorded on a Horiba FluoroMax 4 spectrometer (Horiba, Middlesex, United Kingdom). Polymer solutions were made using chloroform and measured using quartz cuvettes (path length = 1×10^{-2} m). Thin films were prepared by drop-casting solutions onto quartz plates using 5 mg cm^{-3} polymer solutions that were prepared with chlorobenzene. Cyclic voltammograms were recorded using a Princeton Applied

Research Model 263A Potentiostat/Galvanostat (Princeton Applied Research, Cambridge, United Kingdom). A three electrode system was employed comprising a Pt disk, platinum wire, and Ag/AgCl as the working electrode, counter electrode, and reference electrode, respectively. Measurements were conducted in a tetrabutylammonium perchlorate acetonitrile solution (0.1 mol dm^{-3}) on polymer films that were prepared by drop casting polymer solution. Ferrocene was employed as the reference redox system, in accordance with International Union of Pure and Applied Chemistry's recommandations.[44]

1,3-Dibromo-5-(4-butylphenyl)thieno[3,4-c]pyrrole-4,6-dione ***(M3)***

THF (12 cm^3) was added to a round bottom flask containing 4,6-dibromothieno[3,4-c]furan-1,3-dione (1.50 g, 4.81 mmol) and 4-butylaniline (789 mg, 5.29 mmol). The mixture was heated to 50°C for 3 hr. Upon completion, the reaction mixture was cooled to room temperature. Thionyl chloride (5 cm^3) was added, and the reaction was stirred at 55°C for a further 4 hr. The reaction was precipitated into methanol (150 cm^3). The product was filtered off and washed with methanol to give the title compound as white needles (1.73 g, 3.9 mmol, 81%). ^{1}H NMR (400 MHz, $CDCl_3$): ∂ (ppm) 7.31 (d, J = 8.56 Hz, 2H), 7.27 (d, J = 8.56 Hz, 2H), 2.67 (t, J = 7.76 Hz, 2H), 2.67 (m, 2H), 1.39 (h, J = 7.74 Hz, 2H), 0.96 (t, J = 7.32 Hz, 3H). ^{13}C NMR (400 MHz, $CDCl_3$): ∂ (ppm) 159.41, 143.54, 129.08, 129.00, 126.18, 113.92, 35.35, 33.36, 22.34, 13.90. EI-MS (*m/z*): $[M]^+$ calculated for $C_{16}H_{13}Br_2NO_2S$, 440.9028; found, 440.9047. Anal. Calculated for $C_{16}H_{13}Br_2NO_2S$: C, 43.37; H, 2.96; N, 3.16; Br, 36.06; S, 7.23; found: C, 43.31; H, 2.90; N, 3.11; Br, 36.18; S, 7.20.

2,6-Bis-(4,4,5,5-tetramethyl-1,3,2-dioxaborolan-2-yl)-9,10-bis(triisopropylsilylacetylene) anthracene ***(M4)***

A flask containing 2,6-dibromo-9,10-bis(triisopropylsilylacetylene)-anthracene (3.00 g, 4.3 mmol), bis(pinacolato)diboron (3.83 g, 15.01 mmol), potassium acetate (2.52 g, 24.97 mmol), and Pd (dppf)Cl_2 (0.2 g, 0.25 mmol) was placed under an argon atmosphere using standard schlenk line techniques. To this mixture, DMF (50 cm^3) was added, degassed, and heated at 90°C for 48 hr. The reaction mixture was cooled to room temperature, poured into water (50 cm^3), and extracted with diethyl ether (3 × 100 cm^3). The organic phases were combined, washed with H_20 (2 × 100 cm^3), and dried ($MgSO_4$). The crude product was purified by dissolving in the minimum amount of hot ether and precipitation in methanol that had been run through a basic alumina column to afford the product as a yellow powder. (1.41 g, 1.8 mmol, 42%). ^{1}H NMR (400 MHz, $CDCl_3$): ∂ (ppm) 9.30 (s, 2H) 8.62 (d, 2H, J = 8.48 Hz), 7.94 (dd, 2H, J = 0.98 Hz and J = 8.48 Hz), 1.41 (s, 24H), 1.32 (m, 42H). ^{13}C NMR (250 MHz, $CDCl_3$): ∂ (ppm) 136.42, 133.44, 132.37, 130.61, 126.91, 105.22, 103.33, 83.93, 25.00, 18.94, and 11.58. EI-MS (*m/z*): $[M]^+$ calculated for $C_{48}H_{72}B_2O_4Si_2$ 790.515529, found: 790.513046. Anal. Calculated for $C_{48}H_{72}B_2O_4Si_2$: C, 72.90; H, 9.18. Found: C, 73.22; H, 7.72.

Poly[9,10-bis(triisopropylsilylacetylene)anthracene-2,6-diyl-alt-5-(octyl)thieno[3,4-c]pyrrole-4,6-dione] ***[PTATPD(O)]***

2,6-Bis-(4,4,5,5-tetramethyl-1,3,2-dioxaborolan-2-yl)-9,10-bis(triis opropylsilylacetylene) anthracene (**M4**) (0.299 g, 0.378 mmol) and **M1** (0.160 g, 0.378 mmol) were added to a round bottom flask and placed under an inert atmosphere of argon using standard Schlenk line techniques. Anhydrous THF (8 cm^3) and a saturated $NaHCO_3$ (2 cm^3, previously degassed) was added, and the system degassed again. $Pd(OAc)_2$ (6.1 mg, 27.2 μmol) and tri (*o*-tolyl)phosphine (16.4 mg, 53.9 μmol) was added, and the reaction was degassed again. The polymerization was left for 24 hr. Upon completion, the mixture was cooled to room temperature, and bromobenzene (0.15 cm^3, 0.94 mmol) was added. The mixture was degassed and heated to 90°C for 1 hr. Upon completion, the reaction was cooled to room temperature and phenyl boronic acid (150 mg, 1.23 mmol) was added. The mixture was degassed and heated at 90°C for 1.5 hr. The mixture was cooled to room temperature, precipitated in methanol, and left to stir overnight. The polymer was filtered through a membrane and subject to Soxhlet extraction with solvent in the following order: methanol, acetone, hexane, and toluene. The toluene fraction was concentrated *in vacuo* and precipitated in methanol (500 cm^3). The resulting precipitate was stirred overnight and the bright red solid collected by filtration (245 mg, 0.306 mmol, 81%). GPC: toluene fraction, M_n = 27,300 g mol^{-1}, M_w = 74,600 g mol^{-1}, Polydispersity index, *PDI* = 2.73. ^{1}H NMR (500 MHz, $C_2D_2Cl_4$): ∂ (ppm) 9.53 (s, 2H), 8.83 (d, J = 7.48 Hz, 2H), 8.44 (d, J = 7.63 Hz, 2H) 3.75 (br, 2H), 1.79 (br, 2H), 1.50–1.25 (m, 52H), 0.91 (s, 3H). Anal. Calculated for $C_{50}H_{65}NO_2SSi_2$: C, 75.04; H, 8.19; N, 1.75; S, 4.01; found: C, 75.08; H, 8.13; N, 1.66; S, 3.87.

Poly[9,10-bis(triisopropylsilylacetylene)anthracene-2,6-diyl-alt-5-(3,7-dimethyloctyl)thieno[3,4-c]pyrrole-4,6-dione] ***[PTATPD(DMO)]***

PTATPD(DMO) was synthesized according to the polymerization method outline in PTATPD(O). **M4** (0.299 g, 0.378 mmol) and **M2** (0.171 g, 0.378 mmol) were added to a round bottom flask and placed under an inert atmosphere of argon using standard Schlenk line techniques. Anhydrous THF (8 cm^3) and a saturated $NaHCO_3$ (2 cm^3, previously degassed) were added, and the system degassed again. $Pd(OAc)_2$ (6.2 mg, 27.6 μmol) and tri(*o*-tolyl)phosphine (16.3 mg, 53.6 μmol) were added, and the reaction was degassed again. The polymerization was left for 24 hr. The polymer was obtained as a bright red solid (130 mg, 0.157 mmol, 42%). GPC: toluene fraction, M_n = 40,900 g mol^{-1}, M_w = 106,700 g mol^{-1}, *PDI* = 2.61. ^{1}H NMR (500 MHz, $C_2D_2Cl_4$): ∂ (ppm) 9.51 (s, 2H), 8.81 (d, J = 8.09 Hz, 2H), 8.43 (d, J = 8.69 Hz, 2H), 3.75 (br, 2H), 1.81 (br, 1H), 1.59 (m, 3H), 1.48–1.20 (m, 48H), 1.04 (d, J = 5.80 Hz, 3H), 0.90 (d, J = 6.56 Hz, 6H). Anal. Calculated for $C_{52}H_{69}NO_2SSi_2$: C, 75.40; H, 8.40; N, 1.69; S, 3.87; found: C, 76.31; H, 8.79; N, 1.39; S, 3.25.

Poly[9,10-bis(triisopropylsilylacetylene)anthracene-2,6-diyl-alt-5-(4-butylphenyl)thieno[3,4-c]pyrrole-4,6-dione] ***[PTATPD(BP)]***

PTATPD(BP) was synthesized according to the polymerization method outline in PTATPD(O). **M4** (0.299 g, 0.378 mmol) and **M3** (0.168 g, 0.378 mmol) were added to a round bottom flask and placed under an inert atmosphere of argon using standard Schlenk line techniques. Anhydrous THF (8 cm^3) and a saturated $NaHCO_3$ (2 cm^3, previously degassed) were added, and the system degassed again. $Pd(OAc)_2$ (6.0 mg, 26.7 μmol) and tri(*o*-tolyl)phosphine (16.3 mg, 53.6 μmol) were added, and the reaction was degassed again. The polymerization was left for 24 hr. The polymer was obtained as a bright red solid (158 mg, 0.193 mmol, 51%). GPC: toluene fraction, M_n= 25,900 g mol^{-1}, M_w = 97,700 g mol^{-1}, *PDI* = 3.77. ^{1}H NMR (500 MHz, $C_2D_2Cl_4$): ∂ (ppm) 9.59 (s, 2H), 8.81 (m, 2H), 8.46 (d, J = 7.48 Hz, 2H), 7.36 (s, 4H), 2.72 (br, 2H), 1.70 (br, 2H), 1.49–1.20 (m, 44H), 0.99 (t, J = 7.02 Hz, 3H). Anal. Calculated for $C_{52}H_{61}NO_2SSi_2$: C, 76.14; H, 7.50; N, 1.71; S, 3.91; found: C, 76.10; H, 7.49; N, 1.58; S, 3.79.

Acknowledgements

We thank the University of Sheffield (studentship for L. C.) and EPSRC, Grant number EP/M506618/1, (studentship for N. J. R.) for support of this work.

REFERENCES

[1] Y. Xu, F. Zhang, X. Feng, *Small* **2011**, *7*, 1338.
[2] A. K. A. de Almeida, J. M. M. Dias, A. Julia, C. Silva, M. Navarro, S. A. Junior, J. Tonholo, A. S. Ribeiro, *Synth. Met.* **2013**, *171*, 45.
[3] M. Ikai, S. Tokito, Y. Sakamoto, T. Suzuki, Y. Taga, *App. Phys. Lett.* **2010**, *156*, 1.
[4] B. S. Su, E. Gonmori, H. Sasabe, J. Kido, *Adv. Mater.* **2008**, *20*, 4189.
[5] B. C. Krummacher, V. Choong, M. K. Mathai, S. A. Choulis, F. So, F. Jermann, T. Fiedler, M. Zachau, B. C. Krummacher, V. Choong, M. K. Mathai, *Appl. Phys. Lett.* **2006**, *88*, 113506.
[6] S. Reineke, F. Lindner, G. Schwartz, N. Seidler, K. Walzer, B. Lussem, K. Leo, *Nature* **2009**, *459*, 234.
[7] S. G. Robinson, M. C. Lonergan, R. H. Mitchell, *J. Org. Chem.* **2009**, *74*, 6606.
[8] A. Yassar, F. Garnier, H. Jaafari, M. Frigoli, C. Moustrou, A. Samat, R. Guglielmetti, *Appl. Phys. Lett.* **2002**, *80*, 4297.
[9] T. Umeyama, H. Imahori, *J. Mater. Chem. A.* **2014**, *2*, 11545.
[10] H. Sirringhaus, *Adv. Mater.* **2014**, *26*, 1319.
[11] Q. Ling, D. Liaw, C. Zhu, D. S. Chan, E. Kang, K. Neoh, *Prog. Polym. Sci.* **2008**, *33*, 917.
[12] Y. Cheng, S. Yang, C. Hsu, *Chem. Rev.* **2009**, *109*, 5868.
[13] P. M. Beaujuge, J. R. Reynolds, *Chem. Rev.* **2010**, *110*, 268.
[14] R. S. Ashraf, I. Meager, M. Nikolka, M. Kirkus, M. Planells, B. C. Schroeder, S. Holliday, M. Hurhangee, C. B. Nielsen, H. Sirringhaus, I. Mcculloch, *J. Am. Chem. Soc.* **2015**, *137*, 1314.
[15] M. Ak, M. Sulak, G. Kurtay, M. Güllü, L. Toppare, *Solid State Sci.* **2010**, *12*, 1199.
[16] D. T. Mcquade, A. E. Pullen, T. M. Swager, *Chem. Rev.* **2000**, *100*, 2537.
[17] B. Adhikari, S. Majumdar, *Prog. Polym. Sci.* **2004**, *29*, 699.
[18] X. Guo, M. Baumgarten, K. Müllen, *Prog. Polym. Sci.* **2013**, *38*, 1832.
[19] C. M. Amb, S. Chen, K. R. Graham, J. Subbiah, C. E. Small, F. So, J. R. Reynolds, *J. Am. Chem. Soc.* **2011**, *133*, 10062.
[20] S. H. Park, A. Roy, S. Beaupre, S. Cho, N. Coates, J. S. Moon, D. Moses, M. Leclerc, K. Lee, A. J. Heeger, *Nat Phot.* **2009**, *3*, 297.
[21] H. Zhou, L. Yang, W. You, *Macromolecules* **2012**, *45*, 607.
[22] Y. Zou, A. Najari, P. Berrouard, S. Beaupre, B. R. Aïch, Y. Tao, M. Leclerc, *J. Am. Chem. Soc.* **2010**, *132*, 5330.
[23] A. Pron, P. Berrouard, M. Leclerc, *Macromol. Chem. Phys.* **2013**, *214*, 7.
[24] B. Y. Liang, Z. Xu, J. Xia, S. Tsai, Y. Wu, G. Li, C. Ray, L. Yu, *Adv. Mater.* **2010**, *22*, E135.
[25] C. M. Amb, S. Chen, K. R. Graham, J. Subbiah, C. E. Small, F. So, J. R. Reynolds, *J. Am. Chem. Soc.* **2011**, *133*, 10062.
[26] T. Chu, J. Lu, S. Beaupr, Y. Zhang, J. Pouliot, S. Wakin, J. Zhou, M. Leclerc, Z. Li, J. Ding, Y. Tao, *J. Am. Chem. Soc.* **2011**, *133*, 4250.
[27] C. E. Small, S. Chen, J. Subbiah, C. M. Amb, S. Tsang, T. Lai, J. R. Reynolds, F. So, *Nat. Photonics.* **2011**, *6*, 115.
[28] Q. Wu, M. Wang, X. Qiao, Y. Xiong, Y. Huang, X. Gao, H. Li, *Macromolecules* **2013**, *46*, 3887.
[29] J. Y. Back, T. K. An, Y. R. Cheon, H. Cha, J. Jang, Y. Kim, Y. Baek, D. S. Chung, S. Kwon, C. E. Park, Y. Kim, *ACS Appl. Mater. Interfaces* **2015**, *7*, 351.
[30] Y. Li, T. Kim, Q. Zhao, E. Kim, S. Han, Y. Kim, J. I. N. Jang, S. Kwon, *J. Polym. Sci. A. Polym. Chem.* **2008**, *46*, 5115.
[31] C. Liu, W. Xu, X. Guan, H. Yip, X. Gong, F. Huang, Y. Cao, *Macromolecules* **2014**, *47*, 8585.
[32] J. Park, S. Chung, H. Lee, H. Kong, H. Jung, M. Park, S. Cho, C. Eon, H. Shim, *Chem. Commun.* **2010**, *46*, 1863.
[33] M. S. Almeataq, H. Yi, S. Al-Faifi, A. A. B. Alghamdi, A. Iraqi, N. W. Scarratt, T. Wang, D. G. Lidzey, *Chem. Commun.* **2013**, *49*, 2252.
[34] B. Qu, D. Tian, Z. Cong, W. Wang, Z. An, C. Gao, Z. Gao, H. Yang, L. Zhang, L. Xiao, Z. Chen, Q. Gong, *J. Phys. Chem. C* **2013**, *117*, 3272.
[35] Y. J. Kim, K. H. Park, J. Ha, D. S. Chung, Y. Kim, C. E. Park, *Phys. Chem. Chem. Phys.* **2014**, *16*, 19874.
[36] J. Kim, B. Park, F. Xu, D. Kim, J. Kwak, *Energy Environ. Sci.* **2014**, *7*, 4118.
[37] W. A. Braunecker, Z. R. Owczarczyk, A. Garcia, N. Kopidakis, R. E. Larsen, S. R. Hammond, D. S. Ginley, D. C. Olson, *Chem. Mater.* **2012**, *24*, 1346.
[38] A. Najari, P. Berrouard, C. Ottone, M. Boivin, Y. Zou, D. Gendron, W. Caron, P. Legros, C. N. Allen, S. Sadki, M. Leclerc, *Macromolecules* **2012**, *45*, 1833.
[39] B. D. Mühlbacher, M. Scharber, M. Morana, Z. Zhu, D. Waller, R. Gaudiana, C. Brabec, *Adv. Mater.* **2006**, *18*, 2884.
[40] B. Y. Li, Y. Wu, P. Liu, M. Birau, H. Pan, S. Ong, *Adv. Mater.* **2006**, *18*, 3029.
[41] J. Warnan, C. Cabanetos, A. Labban, M. R. El Hansen, C. Tassone, M. F. Toney, P. M. Beaujuge, *Adv. Mater.* **2014**, *26*, 4357.
[42] C. Piliego, T. W. Holcombe, J. D. Douglas, C. H. Woo, P. M. Beaujuge, J. M. J. Fréchet, *J. Am. Chem. Soc.* **2010**, *132*, 7595.
[43] J. Park, D. S. Chung, J. Park, T. Ahn, H. Kong, Y. K. Jung, J. Lee, M. H. Yi, C. E. Park, S. Kwon, H. Shim, *Org. Lett.* **2007**, *9*, 2573.
[44] G. Gritzner, *Pure Appl. Chem.* **1990**, *62*, 1839.

SUPPORTING INFORMATION

Supporting information may be found in the online version of this paper.